THE INFLUENCE OF CARBONACEOUS MATERIAL ON THE MELTING BEHAVIOUR OF MOLD POWDER

D. Singh, P. Bhardwaj, Ying Dong Yang & Alex McLean
University of Toronto, Canada

M. Hasegawa & Masa Iwase
Kyoto University, Japan

ABSTRACT

The melting behaviour of mold powder during continuous casting is an important consideration with respect to caster performance, production rate and steel quality. In this experimental study the effect of different carbonaceous materials on the melting characteristics of mold powders was evaluated. Using X-ray diffraction, different types of carbon were quantitatively characterized in terms of their internal structure and reactivity experiments were conducted to investigate potential relationships between the structural morphology of carbons and their reactivity. High temperature microscopy and drip test experiments were then used to investigate the melting behaviour of mold powders containing different carbonaceous materials. From the results obtained, correlations were established between the structural factors, chemical reactivity and melting behaviour.

INTRODUCTION

Mold fluxes or mold powders are synthetic slags used to cover the liquid steel meniscus during the continuous casting of steel. The fluxes, which are continuously fed on to the surface of the liquid pool during casting, melt first and then the liquid flux flows into the gap between the mold wall and the solidifying steel strand. It is well known that the performance of the flux can greatly affect both the casting operation and product quality. Because of the importance of the flux, intensive investigations have been performed, and considerable progress has been made [1, 2, 3, 4, 5, 6]. The flux above the liquid-steel meniscus generally consists of up to four layers:

- An unreacted, unmelted, dark powder layer on the top
- A sintered, semi-reacted layer
- A mushy zone in which the mold powder is melting
- A molten liquid or slag layer directly over the steel.

The flux layer in the mold/strand gap below the meniscus consists of a solid film that is directly in contact with the mold wall and a liquid film that is in contact with the strand surface. Also, a flux rim, which is often called slag rope or snake, is formed near the top of the meniscus, and this multiphase, wedge-like crust, can greatly affect the down-flow of liquid flux and therefore the casting operation [5, 6]. The main functions of mold flux are:

- Lubrication
- Uniform heat transfer
- Thermal insulation
- Chemical protection
- Inclusion absorption.

Lubrication and uniform heat transfer are probably the most important functions of a mold flux. The mold flux must act to provide a lubricating film between the solidifying shell and the water-cooled mold wall. The lubrication process is complicated and depends on many factors. Fluxes with lower viscosity and/or melting temperatures tend to provide lower friction and better lubrication properties, and thus prevent sticking. Lower melting temperatures mean that liquid flux is present over a greater fraction of the mold length before solidifying alongside the cooling steel shell, therefore providing a greater potential for hydrodynamic lubrication [5, 6, 7, 8]. An even heat flow is necessary to prevent non-uniform solidification of the steel shell, which can lead to cracking of the cast product. Heat transfer strongly influences the occurrence of surface defects during the initial solidification of the steel in the mold. The gap between the mold wall and steel strand can make the heat transfer hard to control. To minimize this gap, a constant and sufficient supply of liquid flux is essential. Therefore, the mold flux melting properties that govern this behaviour are crucial in the selection of mold powders for the optimization of continuous casting.

The melting temperatures of mold fluxes are mainly determined by their chemical and mineral composition, while the melting rate is related to the quantity and type of carbon in the flux. At the present time it is accepted that for a given mineralogical composition of mold powder, the carbon type, amount and particle size primarily determine the melting behaviour. However, there is no evidence in the literature that any attention has been given to the investigation of the relative amounts of amorphous and crystalline structures present in the carbonaceous materials together with their combustion reactivity and the correlation of these parameters with melting behaviour.

To investigate these aspects, a novel approach has been employed that involves quantitative X-ray diffraction analysis (QXRDA), evaluation of combustion reactivity using a

fixed bed reactor, and determination of the melting behaviour of mold powders using high temperature cell microscopy and a drip-test furnace facility. The research has been directed towards evaluation of the structural characteristics of different carbonaceous materials. The relationship between these parameters and the combustion reactivity of the different materials was then determined and this information subsequently correlated with the melting behaviour of mold powders.

METHODOLOGY

Structural Characterization of Different Carbonaceous Materials

Six carbonaceous materials, identified as synthetic graphite, vein graphite, expandable graphite, AG graphite, petroleum coke and metallurgical coke, were studied with respect to their structural properties. A Philips PW1830 X-ray diffractometer with X'Pert software was used to characterize the internal structure of the various carbon samples. The XRD patterns permitted quantification of the amorphous and the crystalline fractions of the carbon samples using a software program developed by Sahajwalla and her Group at the University of New South Wales [9]. The peak width provided an estimate of crystallite height (L_C).

Combustion Reactivity of Different Carbonaceous Materials

Experiments were carried out using a fixed bed reactor to measure the activation energy of various carbon samples during their combustion with a 20%O_2-80%N_2 gas mixture, Figure 1.

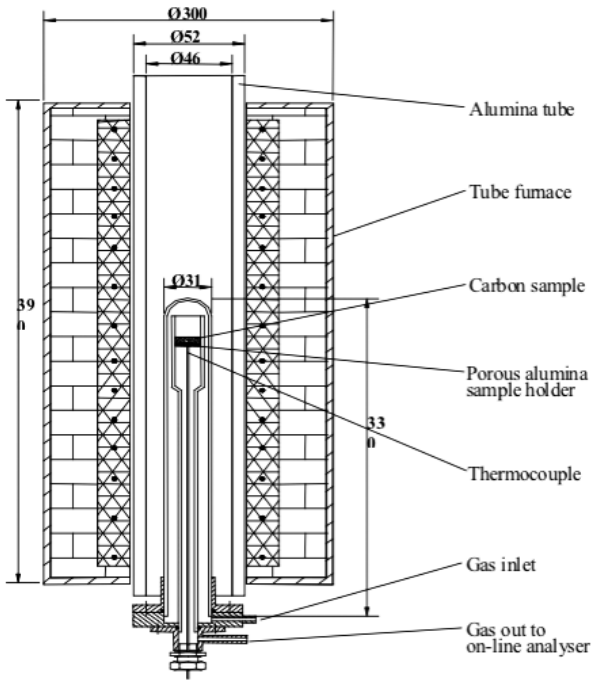

Figure 1: Schematic diagram of the fixed bed reactor

About 0.02 g of the carbonaceous material was placed on a porous alumina plate located inside a quartz tube. The bed temperature was controlled by an S type thermocouple, placed within the sample. The temperature for reactivity measurements was varied from 200°C to 600°C in steps of about 30 degrees. During the experiments, the oxygen-nitrogen gas mixture flows through the bed of carbonaceous material and as the reaction takes places, the gas product containing CO and CO_2 exits through the porous alumina plate into an online infrared gas analyzer where the compositions of the gas mixture can be determined.

Measurement of Melting Temperatures using High Temperature Microscope

The experimental equipment used to measure the melting temperatures of mold powders, Figure 2, consists of a furnace cell with a platinum wire heating element, a programmable power input control unit, and a microscope equipped with a video recording device. The temperature of the reaction cell can be well controlled and precise measurement of the temperature near the test sample can be determined. Mold powder samples containing 3.5 wt% of metallurgical coke, petroleum coke, AG graphite, vein graphite, synthetic graphite and expandable graphite were prepared as pellets, 5mm in height and 5mm in diameter, with the aid of a special die. In order to observe the melting behaviour, the mold powder pellet was placed on an alumina plaque and heated at a controlled rate and the dimensional changes recorded. The effect of different carbons on the melting of mold powder was studied in terms of softening point, T_S, hemispherical point (or melting point), T_m, and flowing point, T_f. The softening point is defined as the temperature at which the edges of the pellet become curved or deformed, the hemispherical point is the temperature at which the sample becomes partially molten and takes on a hemispherical shape, and the flowing point is the temperature at which the sample becomes totally molten and starts spreading. An example of how a mold powder pellet changes shape with respect to these specific temperatures is shown in Figure 3. An image acquisition system permits simultaneous measurement of the changes in height, width, area and angle of the melting pellet.

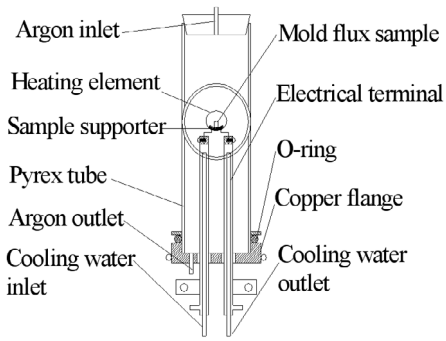

Figure 2: Schematic diagram of the furnace cell for investigation of mold flux melting behaviour

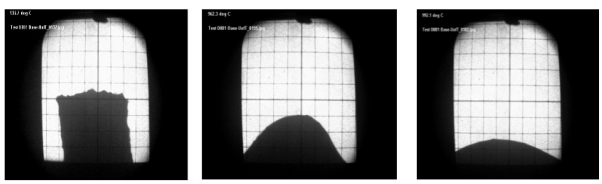

Figure 3: Softening (left), hemispherical (centre) and flowing (right) behaviour of a mold powder

Measurement of Mold Powder Melting Rates

There is no standard method to measure the melting rate of mold flux, although the following methods have been used by different researchers [10]:

- Pyrometric cone or button fusion test
- Quench test
- Molten flux drip test.

The molten flux drip test appears to be the most widely used. A schematic diagram of the drip test facility employed for the present investigation is shown in Figure 4. An induction furnace was used to preheat the bottom of a graphite crucible to a temperature of 1500°C. Mold flux was added to the crucible, and after fusion the liquid flux dripped into a receiver located on the load cell. The weight of the liquid flux produced was continuously recorded on-line with the aid of a computer. The melting rate is defined as the weight of liquid flux produced in unit time.

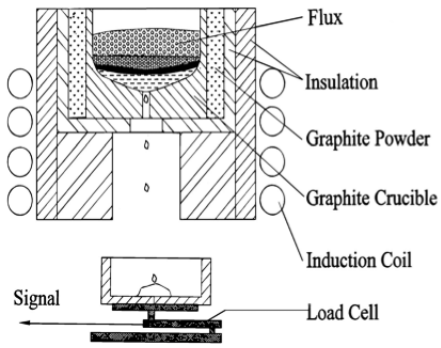

Figure 4: Schematic diagram of molten flux drip test equipment

RESULTS AND DISCUSSION

Structural Aspects of Carbonaceous Materials

The structural parameters of the various carbon samples are presented in Table 1. The experimental results showed that synthetic graphite, vein graphite and expandable graphite had the least amounts of amorphous carbon and therefore the greatest amounts of crystallinity followed by AG graphite, petroleum coke and metallurgical coke. Expandable graphite in original form showed some extra peaks, which were attributed to the intercalation that exists in this material. Once the expandable graphite was heat-treated, the extra peaks disappeared due to the loss of the intercalation material, and the carbon peak was sharper. From crystallite height determinations, vein graphite showed the maximum value followed by AG graphite, expandable graphite, petroleum coke and metallurgical coke.

Table 1: Structural parameters and activation energies of the various carbons

Carbon Type	Amorphous Carbon (%)	Crystallite Height (LC) (Angstrom)	Composite Activation Energy (kJ/mol)	Activation Energy for Amorphous Material (kJ/mol)	Activation Energy for Crystalline Material (kJ/mol)
Synthetic Graphite (SG)	1	-	73	44	158
Vein Graphite (VG)	2	171	72	46	150

Expandable Graphite(EG)	2	88	65	46	170
AG Graphite (AG)	12	124	58	44	160
Petroleum Coke (PC)	18	20	55	42	103
Metallurgical Coke (MC)	21	16	49	42	60

* Note: One Angstrom=0.1nanometer

Combustion Reactivity of Carbonaceous Materials

The reaction rate of carbon, ρ_m (g/g.sec.) was calculated using the amount of CO and CO_2 from the gas analysis and the mass balance for the following chemical reactions:

$$C + ½\ O_2 = CO \quad (1)$$

$$C + O_2 = CO_2 \quad (2)$$

Plotting the reaction rate of the carbon sample against the reciprocal of absolute temperature, a linear relationship would be expected and the gradient of the line should yield a value for the activation energy. For discussion purposes, this value is referred to in the text as the *Composite Activation Energy*. However when plotted in this way, it was found that the reactivity data for all of the materials were in fact slightly curvilinear and could be represented by two straight lines, each with a different gradient. An example of the different representations for vein graphite is shown in Figure 5.

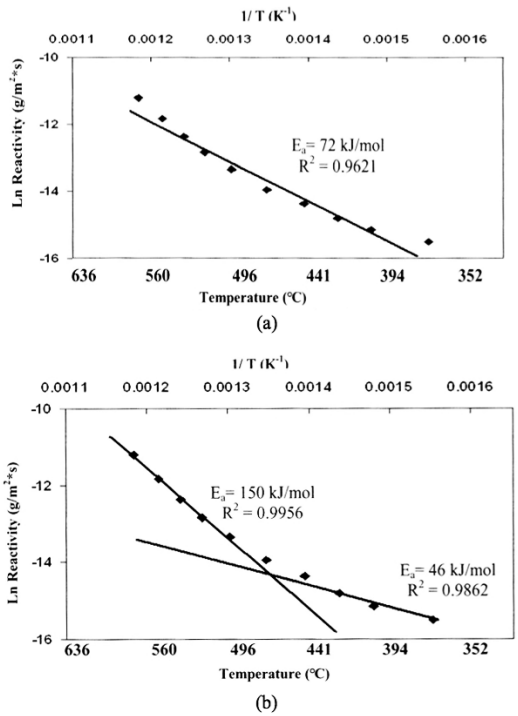

Figure 5: Activation energy plots for vein graphite showing: (a) the composite activation energy and (b) the activation energies for the crystalline and the amorphous structures

In view of the fact that the results from the XRD evaluations show that the carbonaceous materials consist of a mixture of both crystalline and amorphous structures, it would be expected that each of these structures would have a different reactivity. It would seem reasonable therefore that the full reactivity curve can be interpreted in terms of two different regimes, a low temperature regime with a reactivity that corresponds to the amorphous fraction, and a high temperature regime that corresponds to the reactivity of the crystalline fraction. For this reason, the data for each of the lines were analyzed separately. The values of the different activation energies for the various carbon materials are included in Table 1.

It is interesting to note that the activation energy for the amorphous portion was almost the same for all of the different materials. This suggests that the amorphous content present in all of the different carbons is of a similar nature. However within the high temperature regime, which corresponds to the reactivity of the crystalline material, different slopes were observed for the different materials. Comparing the activation energy of various carbons with their amorphous contents and crystallite height values, it can be observed that in most cases the activation energy of carbon increases as the amorphous content decreases and the crystallite height (L_C) increases.

High Temperature Microscopy Measurements

Table 2 shows the softening, hemispherical and flowing points of a mold powder containing four of the different carbons. It can be seen from this table that as carbon is added to the base powder there is an increase in the three characteristic temperatures. There is also an increase in the softening temperature with an increase in the crystallinity of the carbons, Figure 6, and consequently with a decrease in the amorphous content, Figure 7. However, the hemispherical and flowing temperatures are relatively unaffected by changes in the carbon structure. Since these experiments were carried out in a strong oxidizing atmosphere and the amount of carbon present was relatively small, most of the carbon would be oxidized during the initial stages of heating, and the effect of carbon on the hemispherical and flowing temperatures during the later heating would be relatively insignificant.

Table 2: Melting characteristics of mold powder with various carbon additions

	Softening temperature, T_s, °C	Hemispherical Temp, T_m, °C	Flowing Temperature, T_f, °C
BASE	929	954	984
MC	950	973	1003
PC	953	986	1001
AG	955	970	1002
VG	963	970	999

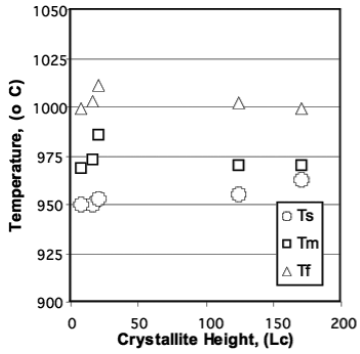

Figure 6: Effect of crystallite height on melting behaviour of mold powder

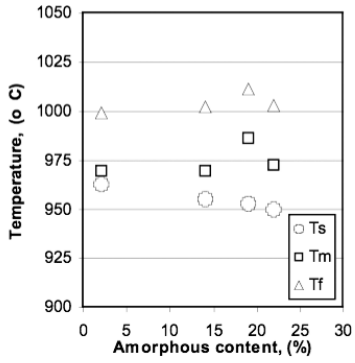

Figure 7: Effect of amorphous content of carbon on melting behaviour of mold powder

Mold Powder Melting Rates

To evaluate the effects of the structural characteristics and reactivities of different carbonaceous materials on the melting behaviour, experiments were conducted with mold powder containing 3.5% of different carbons using the drip test method. It is difficult however, to compare the melting rate values on an absolute scale because of problems in controlling the temperature and temperature gradient across the crucible. For this reason, the melting rates of mold powders with different types of carbon addition are compared with that of the base mold powder without any carbon addition. Examples of the results obtained are shown in Figures 8 and 9.

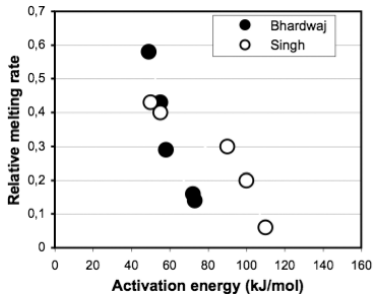

Figure 8: Relative melting rate of mold fluxes vs. composite activation energy

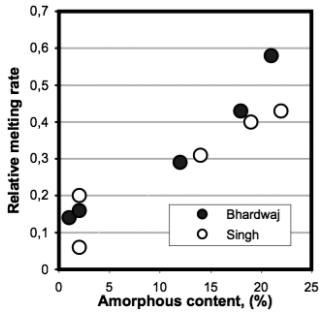

Figure 9: Relative melting rate of mold fluxes vs. amorphous content of carbons

From Figure 8 it can be observed that the melting rate of the mold powder decreases as the composite activation energy of the carbon addition increases. For this reason, mold powder containing vein graphite has the lowest melting rate while the mold powder with metallurgical coke has the highest melting rate. Figure 9 shows the effect of amorphous content of carbon on the melting rate of mold powders. As the amorphous content increases, the melting rate also increases. Thus mold powders with a higher content of amorphous material such as metallurgical coke, show a higher melting rate, compared to mold powders with more crystalline carbons, such as vein graphite. When different carbon materials are exposed to high temperature and oxygen, the amorphous carbon begins to burn off first as it has lower activation energy than the crystalline material. Thus carbons with higher amorphous contents will be consumed more quickly, leaving the unprotected mold powder particles to fuse together and thus complete the melting process sooner. On the other hand, the lower the reactivity of carbon, the lower the melting rate. This is because free carbon provides an inert barrier between the solid particles or liquid flux droplets. Since the carbon particles are not soluble in the liquid flux and are not wetted by the liquid flux, carbon particles form a skeleton that prevents or retards the agglomeration of the liquid droplets. Thus, if the reactivity of the carbon is lower, it will take a longer time for the carbon to oxidize and this will result in a lower melting rate.

CONCLUSIONS

The important findings from this research can be summarized as follows. Carbon with amorphous structure has a low combustion activation energy and high reactivity, while crystalline carbon has a high combustion activation energy and low reactivity. These fundamental parameters have been correlated with the melting characteristics of mold powders. The new knowledge generated on the influence of carbon structure on carbon reactivity and hence on the melting rate of mold powders provides a new basis for the compositional design of powders and this in turn will facilitate the establishment of appropriate casting conditions for different steel grades.

ACKNOWLEDGEMENTS

The authors gratefully acknowledge the financial support received from the Natural Sciences and Engineering Research Council of Canada, Materials and Manufacturing Ontario and Process Research Ortech. Helpful discussions and the provision of mold powder samples by U.S. Steel Canada, formerly Stelco Inc., is also deeply appreciated.

REFERENCES

Branion, R. V. (1987). *Mold Fluxes for Continuous Casting*. Mold Powders for Continuous Casting and Bottom Pour Teeming, Ed. G. Harry, ISS-AIME, pp. 3-14. [1]

Pinheiro, C. A., Samarasekera, I. V. & Brimacombe J. K. (1994). *Mold Flux for Continuous Casting of Steel*. I&SM, October, pp. 55-56. [2]

Heaslip, L. J., McLean, A. & Sommerville, I. D. (1983). *Properties and Performance of Mold Powders*. Continuous Casting, Volume One, ISS-AIME, pp. 113-122. [3]

Mills, K. C. (1985). *Effect of Casting Powder on Heat Transfer in Continuous Casting*. The Metals Society, London, England, pp. 57.1-57.7. [4]

Moore, J. A., Phillips, R. J. & Gibbs, T. R. (1991). *An Overview for the Requirement of Continuous Casting Mold Fluxes*. Steelmaking Conference Proc., ISS-AIME, pp. 615-621. [5]

Chang, H. Y., Lee, T. F. & Ko, Y. C. (1984). *Mold Flux Testing for Continuous Casting of Steel*. ISS Transactions, Vol. 4, pp.27-32. [6]

Nakato, H., Sakuraya, T., Nozaki, T. Emi, T. & Nishikawa, H. (1987). *Physical and Chemical Properties of Casting Powders Affecting the Mold Lubrication during Continuous Casting*. Mold Powders for Continuous Casting and Bottom Pour Teeming, Ed. G. Harry, ISS-AIME, pp. 23-29. [7]

Riboud, P. V. & Larrecq, M. (1983). *Lubrication and Heat Transfer in a Continuous Casting Mold, Continuous Casting*. Volume One, ISS-AIME, pp. 123-125. [8]

Lu, L., Sahajwalla, V., Kong, C. & Harris, D. (2001). *Quantitative X-ray Diffraction Analysis and its Application to Various Coals*. Carbon, 39, pp. 1821-1833. [9]

Xie, B., Wu, J. & Gan, Y. (1991). *Study on Amount and Scheme of Carbon Mixed in CC Mold Fluxes*. Steelmaking Conference Proceedings, ISS-AIME, pp. 647-651. [10]